J. Myanmar Acad. Arts Sci. 2021 **Vol. XIX. No.5A**

SOIL DEGEAGATION ALONG YANGON-NAYPYIDAW HIGHWAY BETWEEN MILE POST 10 AND 40 IN MYANMAR

Aung Kyaw Myat[1], Day Wa Aung[2] and Hlaing Myo Nwe[2]

Abstract

This research is carried out along Yangon-Naypyidaw Highway between Mile Post 10 and 40 to explore the degradation of soil especially caused by gully erosion. The study area covers along the road with Irrawaddy Formation, Older Alluvium (Lateritic soil) and Younger Alluvium. The top soil layer of study road segment is mainly composed of sand, silt, clay and little gravel of Older Alluvium. This layer consists of loosely consolidated, fine to medium grained silty sand with clay which possess 5-10 numbers of blow count as Standard Penetration Test. Moisture contents of top soil layer comprising cohesionless soil is mainly controlled to land degradation. There are many erosion processes along the study road because of the highly rainfall as well as deforestation. Land degradation is high potential during rainy season. The main causes of human-induced land degradation in this area are expansion of cropland and cutting for fire woods. Soil salinization caused by sodium and potassium elements composing in soil is also one of the main controlling factors for soil degradation in rainy season. Vegetation covered on gully floor is very important to protect soil degradation which can reduce surface erosion. Reforestation should also be made for soil stabilization. In some places, temporary physical structures such as gully reshaping, brushwood, sandbag, loose stone, gabion and arc-weir check-dams should be built to minimize gully erosion.

Keywords: Soil degradation, gully erosion, soil stabilization, Reforestation

Introduction

Soil degradation is among serious prevailing issues in modern era. Soil erosion caused by runoff water is one of the most important land-degradation processes in the world. It is being caused due to natural and anthropogenic activities. The level of degradation depends on the degree of degradative processes; duration of usage of such degraded land and its management.

Location

The study road starts at N 17°04' 00", E 96° 10' 02" and ends at N 17º 24' 46", E 96º 20' 32". This road is 18 km long from Yangon Township, Yangon Region to Phayargyi Township, Bago Region which is shown in Figure (1). This area is located at the southern part of Central Myanmar especially along the eastern part of Bago Yoma.

[1] Dr, Associate Professor, Department of Geology, University of Yangon (aungkyawmyat95@gmail.com)
[2] Dr, Professor and Head, Department of Geology, University of Yangon (dawaaung.geol@gmail.com)
[2] Dr, Associate Professor, Department of Geology, Bago University (hmyonwe@gmail.com)

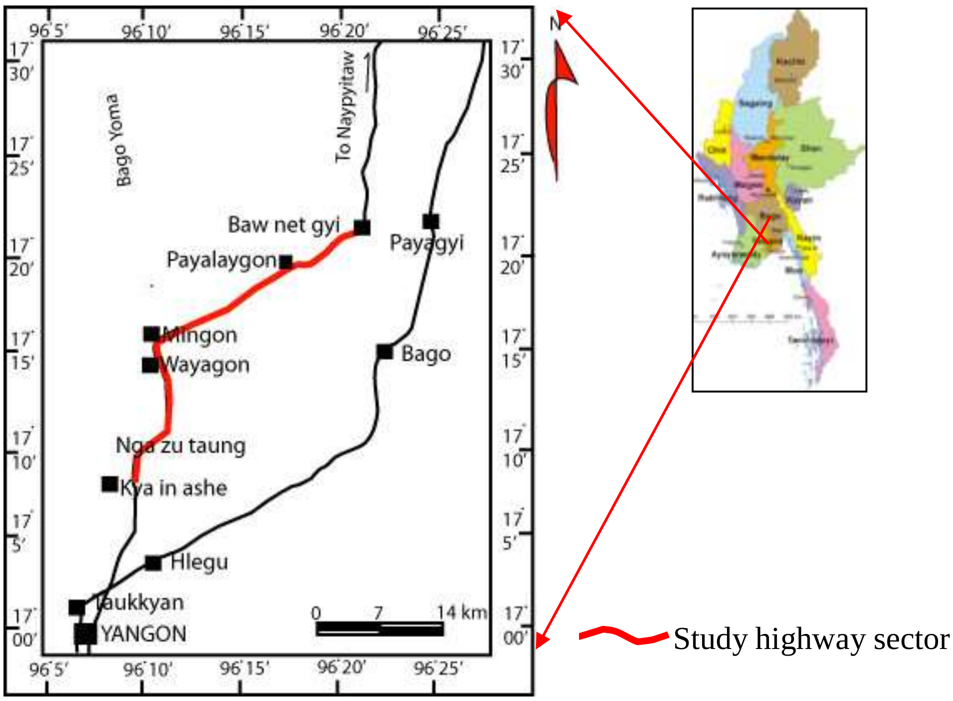

Figure 1 Location map of the study area

Regional Geologic Setting

The study area is located in Inner-Myanmar Tertiary Basin. This basin is divided into sub-basins with Tertiary sediments and uplift areas with older sediments and crystalline rocks, with block faulting and compressional folding of the basin filling. Among these, Bago Yoma is structurally an uplifted range in the Inner-Myanmar Tertiary Basin.

The study area is generally composed of Neogene clastic sedimentary rocks of Kyaukkok Formation (Early Miocene) and Obogon Formation (Middle Miocene), Irrawaddy Formation (Late Miocene to Pliocene), Older Alluvium (Pleistocene) and Younger Alluvium (Holocene). The study area along highway is mainly covered by Irrawaddy Formation, Older Alluvium and Younger Alluvium. Older Alluvium is composed of lateritic soil, silty sand and sandy silt mainly exposed along the road (Figure 2). Younger Alluvium is found as farms and stream sediments which is mainly composed of clayey silt and silty sand. The regional geology of the study area is described in Figure (3).

Figure 2 Residual soil outcrop of Older Alluvium at mile post 15/4

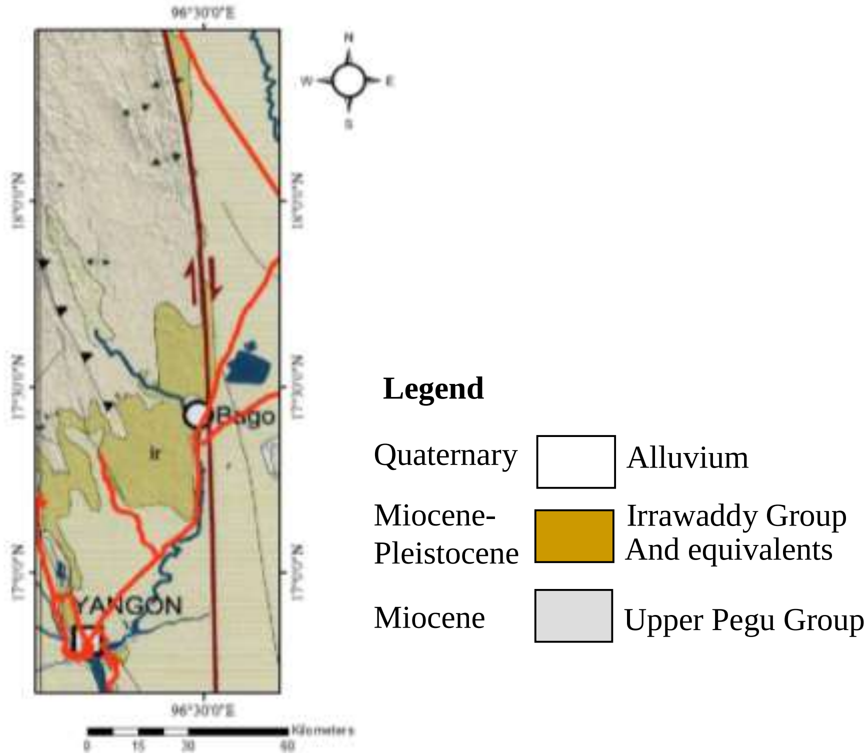

Figure 3 Regional geological map of the study area (MGS, 2014)

Aims and Objectives

The main aim of this research is to explore causes of land degradation by gully erosion and to find out suitable supporting system for that area. Moreover, the objectives of this study are as follows;

- To observe soil erosion along highway
- To explore the process of land degradation
- To identify the control of soil erosion along highway
- To select suitable soil stabilization method

Methodology

Firstly, the literature surveys related to gully erosion and soil degradation such as Ravi and D'Odorico 2005, Pimentel and Burgess 2013 had been made by the authors who described. By using the (Garman 78) GPS, the waypoints are recorded in detail to plot on the google map.

Object-based segmentation and classification of bareland, vegetation and water bodies based on LANDSAT-8 satellite images acquired for the landcover changes of 2017 and 2020 along the road. Assessment of classification accuracy of the land-cover classes is used 600 randomly distributed control points by using field data and google earth images. Quantification of land-cover changes detection overlay-analysis and of net land-cover gains and losses using change cut and fill analysis.

Land erosion and measurement of the cutting slopes have also been made with Brunton compass and distance meter along the highway to measure the length and width of outcrops and gullies. The velocity of water flowage was measured based on flowage meters per second along the gullies.

Geotechnical analysis for land degradation was made in accordance with the field investigation of American Society for Testing and Materials (ASTM D 1586-99/D 2487-98) and laboratory investigation of (ASTM D 2216, D 7263, D 422, D 3080-12).

Collecting soil samples had been made to explore the geochemical behaviors of soils especially salinity along highway. The collected soil samples were tested and analyzed by Atomic Absorption Spectrophotometer (AAS).

Results and Discussions

Land degradation covers the various forms of soil degradation, adverse human impacts on water resources, deforestation, and lowering of the productive capacity of rangelands. This research is carried out based on the study of gully erosion by land cover changes, engineering geological aspects of soil, rainfall effect and geochemistry of soil.

Satellite Image Analysis

Land cover change was made on the application of object-based segmentation and classification techniques using 2017 and 2020 LANDSAT-8 satellite images for the road. It is characterized by a diverse landscape with two major landforms: plains and rolling hills. Rolling Hills cover 40 % of the total area. The land-cover maps produced for 2017 and 2020 are presented in Figure 8, 9 and 10. They show that the overall accuracies of the 2017 and 2020 land-cover maps were 75 % and 85 % respectively. Therefore, the achieved accuracies were considered to be acceptable for quantified change detection analyses.

The whole area of bareland, vegetation and water body areas was shown in Figure (4). According to classification of land cover changes, in 2017-2018, this area is composed of bareland (61.79%), vegetation cover (34.28%) and water body (3.93%). The bareland area changed 1598284.6 km2 and unchanged area was 1065133.1 km2. The vegetation covered area also changed 772290.1 km2 and unchanged area was 705219.2 km2. Besides, water body changes were found in 147247.3 km2 and unchanged water bodies area was 22354.1 km2.

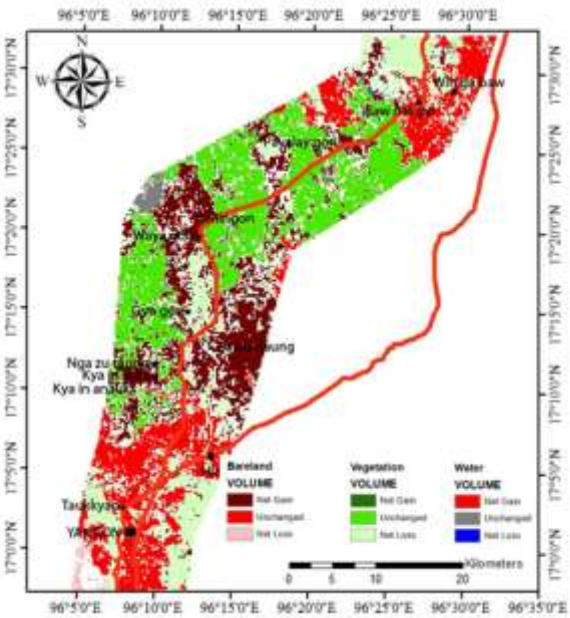

	Gain	
	Area (km^2)	Percent
Water	132,405.2	78.07%
Bareland	1,345,265.3	50.51%
Vegetation	48,981.0	3.32%

	unchange	
	Area (km^2)	Percent
Water	22,354.1	13.18%
Bareland	1,065,133.1	39.99%
Vegetation	705,219.2	47.73%

	loss	
	Area (km^2)	Percent
Water	14,842.1	8.75%
Bareland	253,019.3	9.50%
Vegetation	723,309.1	48.95%

Figure 4 Land cover changes map of satellite imagery in 2017-2018

In 2018-2019, the total areas of bareland (88.89%), vegetation cover (5.81%) and water body (5.30%) were observed which is shown in Figure (5). The bareland area changed 3,164,200.1 km^2 and unchanged area was 667265.5 km^2. The vegetation covered area also changed 140,304.2 km^2 and unchanged area was 667265.5 km^2. Moreover, water body change occurred 203,361.5 km^2 and unchanged water body area was 25,143.2 km^2.

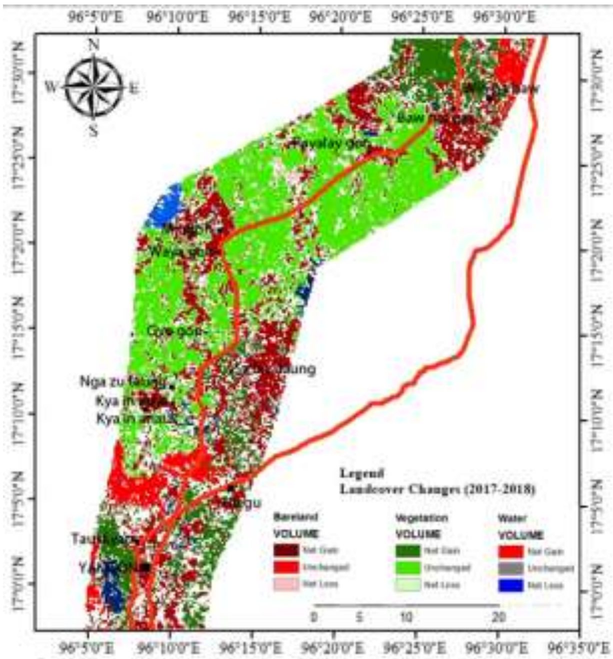

	Gain	
	Area (km^2)	Percent
Water	197,255.2	86.32%
Bareland	2,953,065.0	77.07%
Vegetation	133,528.1	53.29%

	unchange	
	Area (km^2)	Percent
Water	25,143.2	11.00%
Bareland	667,265.5	17.42%
Vegetation	110,254.1	44.01%

	loss	
	Area (km^2)	Percent
Water	6,106.3	2.68%
Bareland	211,135.1	5.51%
Vegetation	6,776.1	2.70%

Figure 5 Land cover changes map of satellite imagery in 2018-2019

According to classification of land cover changes, in 2019-2020, this area is composed of bareland (84.03%), vegetation cover (15.34%) and water body (0.63%) which is shown in Figure (6). The bareland area changed 3,623,348.0 km^2 and unchanged area was 1,235.0 km^2. The vegetation covered area also changed 340,945.2 km^2 and unchanged area was 320,157.1 km^2. Besides, water body change was found in 26,213.2 km^2 and unchanged water bodies area was 1,100.1 km^2.

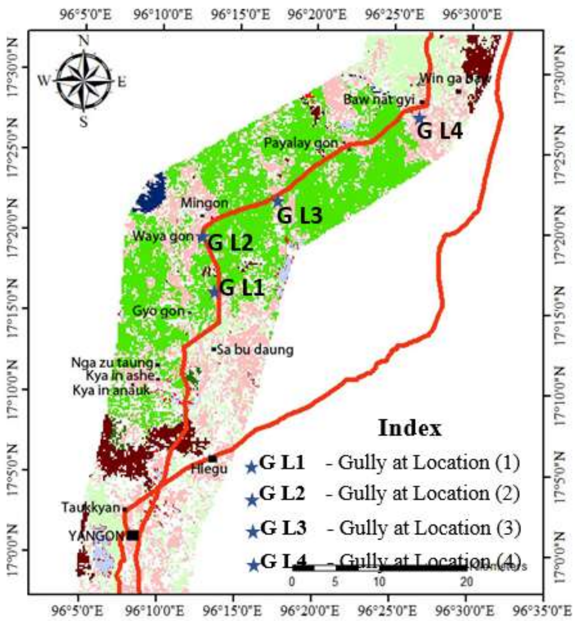

	Gain	
	Area (km^2)	Percent
Water	6,213.1	22.75%
Bareland	522,103.1	14.00%
Vegetation	21,075.1	3.62%

	unchange	
	Area (km^2)	Percent
Water	1,100.1	4.03%
Bareland	1,235.0	0.40%
Vegetation	320,157.1	48.00%

	loss	
	Area (km^2)	Percent
Water	20,000.1	73.22%
Bareland	3,101,244.9	85.60%
Vegetation	319,870.1	48.38%

Figure 6 Land cover changes map of satellite imagery in 2019-2020

According to comparative study of land cover changes from 2017 through 2020, vegetation covered area gradually changed to bareland area in recent year. On the other hand, deforestation is most pronounced in this area.

Case Study

There are many erosion processes along the road segment because of the high rainfall as well as deforestation. High potential land degradation is observed in the central part of the study road mainly occurred in rainy season. Some land degradations related to gully erosions are described in Table (1, 2, 3 & 4) and Figure (7, 8, 9 & 10). The main control of this erosion process is water flowage that the flowage velocity of the channels ranges from 0.25 to 0.7ms^{-1} in raining time. Moreover, the estimate rates of sedimentation also range from 10 % to 25 % per liter in that time. According to field measurement, estimated surface eroded area of gully erosion can be calculated with $A = bh + 2ls + lb$ and estimated eroded volume can also be calculated with $V = ½ (bh)l$.

Table 1 Field measurements of gully erosion at location 1

Loc. 1	Width (b)	Length (l)	Depth (h)	Slope of gully (s)	Eroded area	Estimate volume	Gully Material
Gully A	7 m	60 m	5 m	6.5 m	1235 m^2	1050 m^3	Silty Sand
Gully B	12 m	70 m	7 m	9 m	2184 m^2	2940 m^3	Silty Sand

Table 2 Field measurements of gully erosion at location 2

Loc. 2	Width (b)	Length (l)	Depth (h)	Slope of gully (s)	Eroded area	Estimate volume	Gully Material
Gully A	3 m	70 m	3 m	4 m	779 m^2	315 m^3	Sandy Silt

Table 3 Field measurements of gully erosion at location 3

Loc. 3	Widt h (b)	Lengt h (l)	Dept h (h)	Slope of gully (s)	Eroded area	Estimate volume	Gully Material
Gully A	15 m	75 m	6 m	7.5 m	2340 m^2	2275 m^3	Sandy Silt

Table 4 Field measurements of gully erosion at location 4

Loc. 4	Width (b)	Length (l)	Depth (h)	Slope of gully (s)	Eroded area	Estimate volume	Gully Material
Gully A	4 m	45 m	4 m	4.7 m	619 m^2	360 m^3	Clayey Silt

(A)

(B)

Figure 7 (A) Nature of gully erosion at Gully A (B) Recently eroded nature at Gully B

Figure 8 Nature of gully erosion at Location 2

Figure 9 Gully erosion caused by heavy rainfall at Location 3

Figure 10 Gully erosion caused by heavy rainfall at Location 4

Rainfall Data Analysis

According to rainfall data of (DMH) in Myanmar, rainfall is high in June and July (Figure 11). Highest rainfall occurs in August, 2019 and it is followed by the rainfall of June, 2015 and September, 2016.

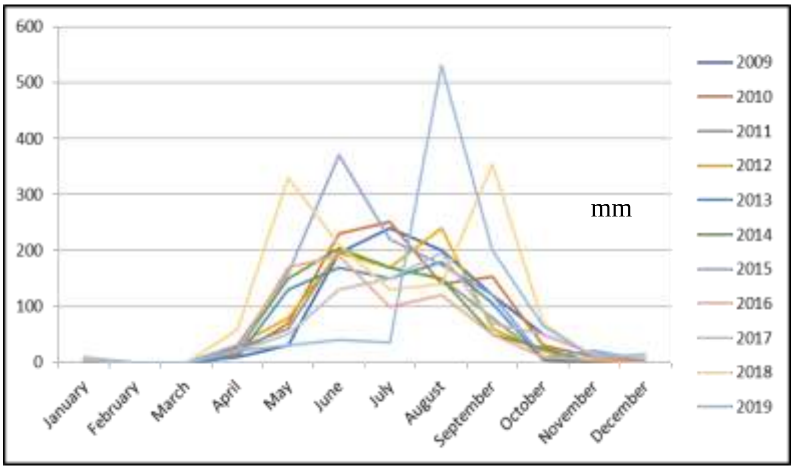

Figure 11 Average rainfall data analysis of the study area

Geotechnical Data Analysis

On the basis of lithologic units, the research area of road segment is mostly composed of loosely consolidated sandstone intercalated with shale and clay of Irrawaddy Formation and laterite deposit of Older Alluvium and rarely found sand, silt, shale, clay and slope wash deposits of Younger Alluvium.

Analysis from Standard Penetration Test Data

The engineering geology of the research road is analyzed on the basis of geology and engineering behavior of soils. This investigation had been done based on the 12 boreholes especially along the road segment. Idealized cross-section of subsurface soil layer is described in Figure (12).

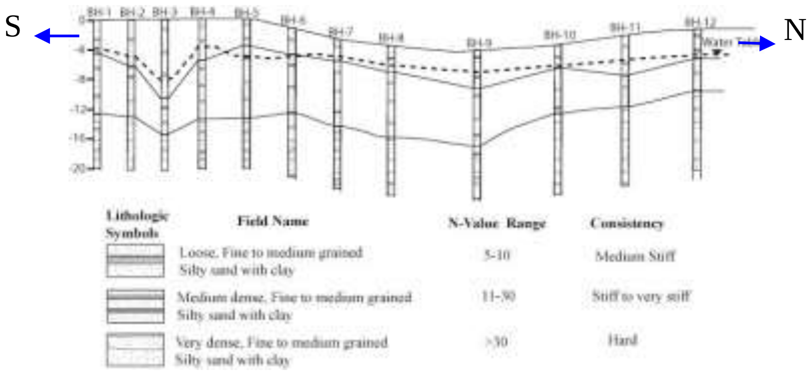

Figure 12 Idealized cross-section of subsurface soil layers on borehole data

According to this study, subsurface soil layer can be classified basically as Top layer composed of loosely consolidated Silty sand, Middle layer made up of medium dense Silty sand and Lower layer composed of very dense Silty sand. Groundwater level contains in Top layer at 3-8 meter depth. Top layer has SPT N-value (5-10) and is composed of loosely consolidated soil layer. Hence, this layer can easily be eroded in external agents such as rain, stream and air.

Grain Size Distribution Analysis

According to the grain size distribution analysis, top soil layer of borehole 2, 5, 10, 11 and 12 is composed of poorly graded silty sand which is a cohesionless soil. It is not suitable for basement as well as for slope stability. Besides, it is also easily erodible in rainy season.

Moisture Content Analysis

Moisture content was used for determining the erosional resistance of top soil layer. These data were measured on two situations such as dry time and wet time or rainy time. According to this analysis, moisture contents of top soil layer have 13 to 28 % generally in normal condition. But in rainy time, moisture contents can contain to 32 to 38 % of total soil condition. This situation points out that the greater the water containing the soil, the more erosion can take place.

Analysis from Direct Shear Test Data

Direct shear test was conducted to determine the strength of soil of the area. The strength measurement parameters are cohesion (c) and angle of internal friction (ϕ) which is described in Table (5).

Table 5 Results of direct shear test for top soil layer of each boreholes

Borehole	**1**	**2**	**3**	**4**	**5**	**6**	**7**	**8**	**9**	**10**	**12**
Cohesion (c) KN/m^2	0.0	0.0	0.0	13.0	18.0	9.8	13.7	13.5	0.0	16.8	9.8
Internal friction (ϕ) degree	34.9	35.1	33.1	32.0	28.1	33.3	31.6	28.2	38.6	31.8	30.1

In this analysis, boreholes 1, 2, 3, and 9 show cohesionless soil condition that can be concluded that top soil layer of these borehole sites assumed as loosely consolidated and poorly graded soil condition.

Engineering Properties of Soils

The top soil layer of study area is mainly composed of sand, silt, clay and little gravel of Older Alluvium. This layer also consists of loosely consolidated, fine to medium grained silty sand with clay as field investigation of boreholes which possess 5-10 numbers of SPT blow count. According to Atterberg's Limit Test (ASTM D 4318), soils of top soil layer can be classified into three different types such as CL, ML and CL-ML. Moreover, moisture contents of top soil layer is different in normal condition and rainy time. This condition is a dangerous condition to erode the top soil where the lack of a ground improvement system prevailed. And the strength of top soil measured by Direct Shear Test indicated that some of top soil layer show cohesionless condition where land degradation processes such gully erosion and small landslides occur in these sites.

Soil Salinity Analysis on Geochemical Data

The elements contained in rocks and minerals are released into the environment by both chemical and physical processes. The geochemical result for these four locations analyzed by AAS is shown in Table (6).

Table 6 Element content in soil samples of location (1-4) (Unit – ppm)

No.	Location	As	Mn	Fe	Na	K	Ca	Mg
1	1	ND	155	8320	165	365	210	190
2	2	ND	185	8320	210	355	190	170
3	3	0.003	225	8150	210	295	275	160
4	4	ND	230	8570	235	380	285	170

According to this result, iron is the main constituent element of soil in this area that has high strength in nature. Sodium, potassium and calcium contain 8-10% in total soils. These elements are soluble in water. Hence, in the rainy season, such elements are dissolve in rain water. In fact, erosion may take place more easily and also degrade the soil.

Proposed Soil Stabilization Methods

It is essential that lands susceptible to gullying should be monitored regularly in early stages of gully formation. It is more suitable to prevent gullies from occurring than to attempt to control them once the erosion has started. Various authors from different countries described soil stabilization methods for gully protections. Among them, the following stabilization methods are suitable for this research area:

(a) Promote revegetation of gully channels to reduce sediment transport capacity with reduction of the slope gradient

(b) Maintain vegetation ground cover on gully features to reduce surface erosion

(c) Some of places should be used with temporary physical structures such as gully reshaping, brushwood, sandbag, loose stone, gabion and arc-weir check-dams.

Conclusions and Recommendations

Soil degradation is among serious prevailing issues in current time. This research is carried out along Yangon-Naypyidaw Highway between Mile Post 10 and 40. This highway does not meet international design, construction and safety standard has seen a spate of accidents since its opening in 2010.

The study road segment is mainly covered by Irrawaddy Formation, Older Alluvium (Lateritic soil) and Younger Alluvium. The construction materials are sand and gravel deposits, laterite, sandstone, granite and gneissic rocks in constructing this highway. Thin gravel beds of the Irrawaddian and Older Alluvium, lateritic soils in the Bago Yoma foot hills contain were also used as construction materials. Sandstone of the Peguan was used for the basement of highway.

There are many erosion processes along the studied highway segment due to high rainfall as well as deforestation. Gullies and sheetwash erosions are pronounced in four locations. Land degradation is potentially high in rainy season.

According to land cover changes of this area from 2017 through 2020, bareland area changes from 61.79 % to 84.03 %, vegetation covered area changes from 34.28% to 15.34% and water body area changes from 3.93 % to 0.63 %.

Moreover, top soil layer along studied road segment is mainly composed of sand, silt, clay and little gravel of Older Alluvium. Moisture contents of top soil layer is mainly changes in normal condition and rainy time which favours the severe erosion of top soil. Some of top soil layer show cohesionless soil condition where land degradation processes such as gully erosion and small landslides occur in these sites.

According to geochemical analysis, soil salinization caused by sodium, potassium and calcium elements containing in soil may accelerate the erosion more easily in rainy season as one of the main control in degradation of soil.

Reforestation is one of the most effective method which can protect erosion of top soil. Some of places should be reinforced with suitable weirs.

Acknowledgements

The authors are also thank to Dr. Myo Thant, Professor, Department of Geology, University of Yangon, for his advices to carry out this research.

The writers are also grateful to Dr. Tun Naing Zaw, Associate Professor of the Department of Geology, University of Yangon for his advices throughout the preparation of this research.

Finallly, we would like to special thanks to U San Oo, Director of Future Soil Technics Co. Ltd., for his valuable geotechnical data of research area.

References

American Society for Testing and Materials, (1998). *Standard Practice for Classification of Soils for Engineering Purposes (Unified Soil Classification System*, D 2487, West Conshohocken, PA 19428 Reprinted from the Annual Book of ASTM Standards, P. 1-11.

American Society for Testing and Materials, (1999). *Standard Test Method for Penetration Test and Split-Barrel Sampling of Soils*, D1586, West Conshohocken, PA 19428 Reprinted from the Annual Book of ASTM Standards, P. 1-5.

American Society for Testing and Materials, (2007). *Standard Test Method for Particle Size Analysis of Soils*, D422, West Conshohocken, PA 19428 Reprinted from the Annual Book of ASTM Standards, P. 1-8.

American Society for Testing and Materials, (2009). *Standard Test Methods for Laboratory Determination of Density (Unit Weight) of Soil* Specimens, D 7263, West Conshohocken, PA 19428 Reprinted from the Annual Book of ASTM Standards, P. 1-7.

American Society for Testing and Materials, (2010). *Standard Test Methods for Laboratory Determination of Water (Moisture) Content of Soil and Rock by Mass*, D2261, West Conshohocken, PA 19428 Reprinted from the Annual Book of ASTM Standards, P. 1-7.

American Society for Testing and Materials, (2012). *Standard Practice for Direct Shear Test of Soils Under Consolidated Drained Condition*, D 3080, West Conshohocken, PA 19428 Reprinted from the Annual Book of ASTM Standards, P. 1-11. Pimentel and Burgess 2013, *Soil Erosion Threatens Food Production*, College of Agriculture and Life Sciences, Cornell University, USA, P. 443-463.

Bieniawski, Z. T., (1989.) *Engineering Rock Mass Classifications*, John Wiley and Sons, New York, 251p.

Pimentel and Burgess (2013), *Soil Erosion Threatens Food Production*, College of Agriculture and Life Sciences, Cornell University, USA, P. 443-463.

Ravi, S., and P. D’Odorico (2005). A field-scale analysis of the dependence of wind erosion threshold velocity on air humidity, Department of Environmental Sciences, University of Virginia, Charlottesville, Virginia, USA, *Geophys. Res*. Lett., Vol. 32, 4p.

Sherwood, P., (1993). *Soil stabilization with cement and lime*. State of the Art Review. London: Transport Research Laboratory, HMSO.